International Geology Review, Vol. 49, 2007, p. 401–415.

Comparative Deformation Behavior of Minerals in Serpentinized Ultramafic Rock: Application to the Slab-Mantle Interface in Subduction Zones

DIANE E. MOORE[1] AND DAVID A. LOCKNER

U. S. Geological Survey, 345 Middlefield Road, MS 977, Menlo Park, California 94025

Abstract

The layer-structure minerals serpentine, brucite, and talc are postulated to form in the mantle wedge above a subducting slab as a result of progressive hydration and silica metasomatism. Tectonic mixing at the slab-mantle interface generates serpentinite mélanges that contain blocks of high-pressure (HP) or ultrahigh-pressure (UHP) metamorphic rock derived from the subducting slab. Such serpentinite mélanges may provide a means of exhumation of HP/UHP metamorphic rocks, and may define the lower limit of locked regions on the subduction interface that fail in large earthquakes. We review recently obtained frictional strength data for brucite and talc over the temperature range 25–400°C at 100 MPa effective normal stress and compare them with new data for antigorite. These minerals respond to heating in different ways, causing their frictional strengths to diverge. Water-saturated antigorite strength increases toward the fixed dry value of $\mu \approx 0.75$–0.80 with heating: $\mu \approx 0.50$ at 25°C and $\mu > 0.60$ at 400°C. The difference in μ between dry and water-saturated talc gouge also decreases with increasing temperature, but both the dry and water-saturated values of μ are lower at elevated temperatures. For dry talc, μ decreases from 0.35 to 0.25 between 25° and 300°C, whereas for water-saturated talc, μ is approximately 0.20 at 25°C and 0.10–0.15 at elevated temperatures. Weakening of the interlayer bond of talc with heating may be responsible for the overall reduction in its frictional strength. The strength of dry brucite also is fixed at $\mu = 0.45$–0.50, but the water-saturated value of μ decreases from ≈ 0.30 at 25°C to 0.20–0.25 at 200°–400°C. The water-saturated brucite gouge has extensively recrystallized along the shear surfaces, and its weakening may be attributable to solution-transfer processes.

Because the serpentine minerals become stronger at elevated temperatures, to achieve low frictional strength in a serpentinized mantle wedge or serpentine-rich mélange would require some other cause such as nearly lithostatic fluid pressures or the addition of lower-strength minerals. Increasing abundance of brucite and talc in serpentinite at constant physical conditions would progressively reduce its frictional strength. The concentration of talc along a metasomatic front at the edge of the mantle wedge or in reaction zones surrounding HP/UHP blocks in serpentinite mélange should tend to localize shear in this extremely weak material.

Introduction

A CONSIDERABLE BODY of evidence exists for hydration of the mantle wedge above subduction zones (see review by Hyndman and Peacock, 2003). Water released from the subducting slab as a result of metamorphic reactions migrates upward into the overlying mantle wedge, causing serpentinization of the ultramafic rocks at temperatures below ~600°C (Manning, 1995). In many cases, a zone of mixing forms at the slab-mantle interface, producing a serpentinite mélange that incorporates pieces of high-pressure (HP) or ultrahigh-pressure (UHP) metamorphic rocks from the subducting slab (e.g., Guillot et al., 2000, 2001; Spaggiari et al., 2002; Dobretsov and Buslov, 2004). Blocks of high-grade blueschist and eclogite in the Franciscan Complex of California typically have rinds of actinolite + chlorite that formed while the blocks were immersed in serpentinite (e.g., Coleman and Lanphere, 1971; Coleman, 1980; Moore, 1984). Such serpentinite mélanges act as a "lubricant" (Guillot et al., 2000) that aids the exhumation of HP and UHP rocks at some convergent margins.

The fluids released from the subducting slab are silica saturated (Manning, 1995), and progressive

[1]Corresponding author; email: dmoore@usgs.gov

Si-metasomatism accompanying hydration of the mantle wedge may lead to a sequence of mineral assemblages beginning with serpentine + brucite, followed first by the conversion of brucite to serpentine and subsequently the replacement of serpentine by talc (Manning, 1995; Peacock and Hyndman, 1999). All three minerals—serpentine, brucite, and talc—have layered crystal structures, and the layer-structure minerals as a group have frictional properties that differ from those of the other common rock-forming minerals (Byerlee, 1978; Morrow et al., 2000; Moore and Lockner, 2004). We have measured the frictional strengths of the serpentine minerals to temperatures of 200–300°C (Moore et al., 1996, 1997, 2004), and we recently completed similar laboratory investigations on brucite and talc to temperatures of 400°C (Moore and Lockner, 2005a, 2005b, and manuscripts in preparation). The serpentine minerals, brucite, and talc have different responses to increasing temperature that affect their frictional strengths. In this paper, we review and compare the frictional strengths of these minerals, in the context of the behavior of layer-structure minerals, and consider the implications for the mechanical behavior of the slab-mantle interface in subduction zones.

Experimental Procedures

New data on antigorite strength at elevated temperatures were obtained for this study, for comparison with talc and brucite. Antigorite ($Mg_{48}Si_{34}O_{85}(OH)_{62}$; Evans, 2004) was the serpentine mineral selected for comparison because, as the high-temperature variety, it is the serpentine mineral most likely to be stable in the hydrated mantle wedge in all but a few cold subduction zones (e.g., Peacock and Hyndman, 1999). All of the experiments at elevated temperatures followed similar procedures, using the furnace assembly illustrated in Figure 1A. Synthetic gouges of the materials to be tested were prepared by hand-grinding the samples and passing them through an 88 μm diameter sieve. Two different antigorite gouges were prepared. One consists of antigorite crystals separated from an antigorite schist from Vermont, obtained from Ward's Scientific. The other is an antigorite-rich serpentinite from New Idria, California, from which veins and altered areas were removed prior to grinding. The latter is the same antigorite-rich gouge that was tested by Moore et al. (1997), and it contains ~76% antigorite, with ~12% magnetite, ~8% calcite, and ~3% chlorite as the principal impurities. The brucite ($Mg(OH)_2$; from Lancaster County, Pennsylvania) and the talc ($Mg_3Si_4O_{10}(OH)_2$; from Balmat, New York) used in the heated experiments are essentially pure mineral separates prepared from specimens obtained from Ward's Scientific. Room-temperature talc experiments were run on a commercial talc powder (Moore and Lockner, 2004).

The sample consists of a 1 mm thick layer of gouge placed along a 30° sawcut in a 19.1 mm diameter cylinder of rock (Fig. 1A). For the antigorite experiments, dunite cylinders were used to avoid reaction with the gouge during the experiments. For the same reason, cylinders of dunite or antigorite serpentinite were the driving blocks for the brucite-gouge experiments. The talc gouge was placed in cylinders of antigorite or granodiorite. The granodiorite cylinders tended to allow more shear displacement before jacket failure than did the serpentinite ones, and talc strength was not affected by the type of driving block used. A borehole for pore-fluid entry was drilled into the upper half of each cylinder (Fig. 1A). The gouge-filled cylinder was placed in an annealed copper jacket between titanium carbide end plugs and Lucalox insulators. The space between the jacketed assembly and the furnace was loosely packed with boron nitride, which is a good thermal and poor electrical conductor. All reported strengths have been corrected for the strength of the jacket, using the revised corrections determined during the investigations on talc (Moore and Lockner, in prep.).

Once in the pressure vessel, confining pressure was applied first to the sample, followed by pore pressure for water-saturated experiments, using deionized water for the pore fluid. The temperature was then raised to the desired value; temperature was monitored by a thermocouple inserted along the pore-pressure inlet. The experiments were all run at a constant normal stress, which was maintained by means of computer-controlled adjustments to the confining pressure. All of the experiments described in this paper were run at 100 MPa effective normal stress, to facilitate comparisons. During an experiment, a piston advanced against the base of the sample column at a specified rate, causing shear in the gouge layer. Axial displacement rates varied between 0.01 and 1.0 μm/s. Axial-displacement and differential-stress values were approximately zeroed before the beginning of the experiment; slight

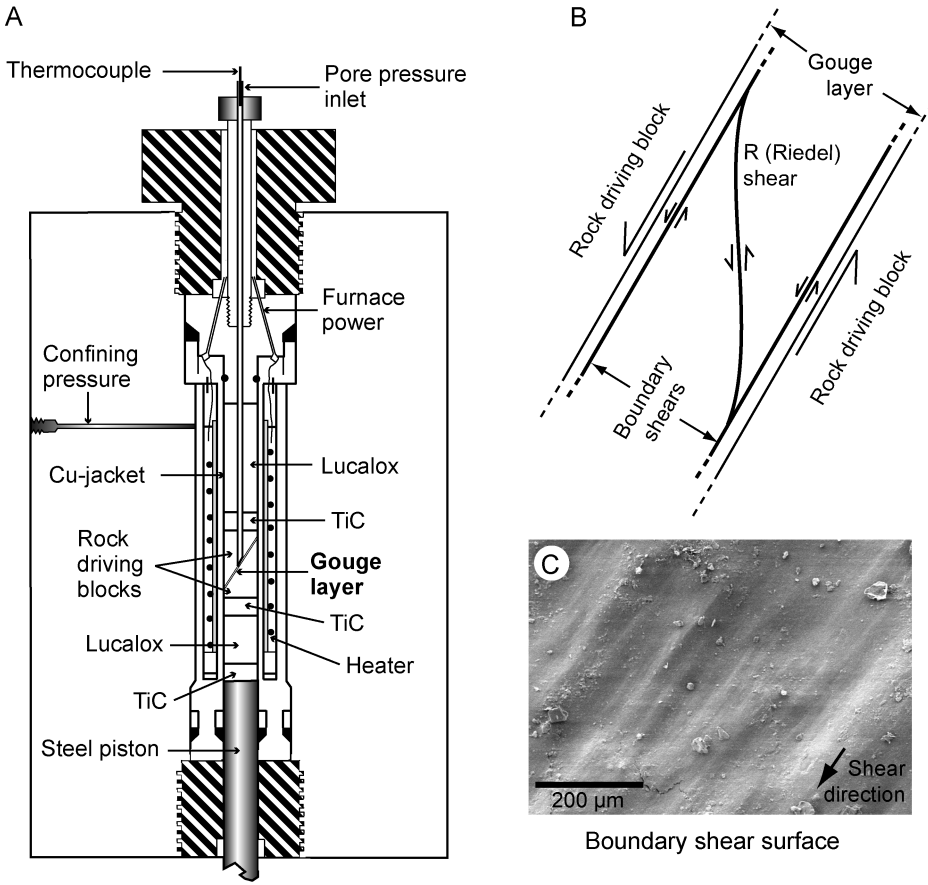

FIG. 1. A. Sample assembly for heated triaxial friction experiments. B. Sketch of the shears typically developed in gouge rich in layer-structure minerals. C. Secondary-electron scanning electron microscope (SEM) photo of one side of a boundary shear developed in talc during shear at room temperature. Arrows on this and other SEM photos indicate the direction of motion of the shear surface.

adjustments were made, as necessary, after the experiment.

The sample assembly and procedures for the room-temperature experiments are similar to those at elevated temperatures. In the absence of the internal furnace, the sample diameter increases to 25.4 mm, which allows for a greater amount of offset than can be achieved during the heated experiments. Polyurethane jackets were used for room-temperature experiments. Both dry and water-saturated frictional strengths were measured. After drying overnight (about 22 hours) at 120°C in a vacuum oven to remove the water adsorbed onto crystal surfaces, the samples were immediately transferred from the oven to the pressure vessel. The samples were sheared dry to 4 mm axial displacement; then, water was introduced to the sample at 10 MPa pressure, and normal stress was raised to keep the effective stress the same as for the dry measurements. The samples were allowed to equilibrate ~60 minutes before shearing was resumed; calculated fluid-saturation times for the gouge layers are ~30 minutes (Moore and Lockner, 2004). The same drying procedures were used for dry friction experiments at elevated temperatures.

In Figure 1B, a portion of the gouge layer is sketched in its orientation in the pressure vessel. Shear displacement within the gouge layer is about 15% greater than the axial displacement. During experiments on gouges rich in layer-structure minerals, shear becomes localized along boundary shears situated near the interfaces with the driving

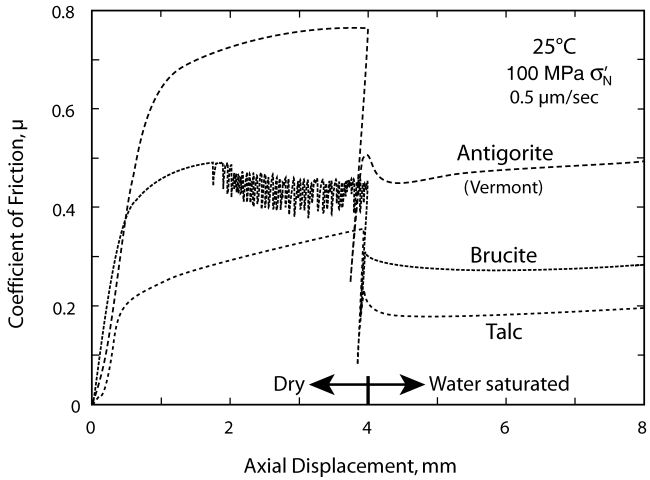

FIG. 2. Dry and water-saturated frictional strengths of Vermont antigorite (Morrow et al., 2000) and brucite and talc (Moore and Lockner, 2004) at 25°C and constant effective normal stress of 100 MPa. Dry brucite is characterized by stick-slip behavior, the sequence of alternating stress drops and recoveries considered to be the laboratory equivalent of earthquakes.

blocks and also along cross-cutting R (Riedel) shears that make small angles (usually <15°; Moore et al., 1989) to the boundary shears and curve into the boundary shears at their junctures. Figure 1C is an example of one of the boundary-shear surfaces from a room-temperature talc experiment. As the shears form, the plates of layer-structure minerals bend and rotate so that the (001) planes are subparallel to the shear orientations. When a sample is disassembled after an experiment, the gouge layer comes apart along the corrugated shear surfaces. The opposite face of the shear shown in Figure 1C has the same appearance but with direction indicators facing the opposite way. Individual R shears do not appear to take up much of the slip, but a given sample typically contains several of them.

Room-Temperature Frictional Strengths

The dry and water-saturated frictional strengths of antigorite, brucite, and talc at room temperature are compared in Figure 2, plotting coefficient of friction, μ, against axial displacement, where μ is defined as follows:

$$\mu = \tau/\sigma_N'$$

(coefficient of friction = shear stress/effective normal stress)

$$\sigma_N' = \sigma_N - P_p$$

(effective normal stress = normal stress – pore-fluid pressure).

The dry frictional strengths of these three minerals differ markedly, dry antigorite being strong and dry talc relatively weak. Lizardite (Morrow et al., 2000) and chrysotile (Moore at al., 2004) have dry strengths similar to that of antigorite. Adding water has a pronounced lubricating effect on these minerals; nevertheless, water-saturated antigorite is considerably stronger than either brucite or talc.

The dry frictional strengths of the layer-structure minerals are useful for understanding their behavior. Gouges of minerals such as quartz, feldspar, calcite, and laumontite have μ ~ 0.8 at 100 MPa effective normal stress, whether dry or wet (Morrow et al., 2000). This value of μ ~ 0.8 at room temperature is typical for most of the common rock-forming minerals other than the layer silicates (Byerlee, 1978). Under dry conditions, a few of the layer-structure minerals—such as those with relatively strong interlayer, (001), bonds—are in fact as strong as feldspar, quartz, olivine, and pyroxene (Fig. 3A).

Giese (1978, 1980) and Bish and Giese (1981) calculated the electrostatic component of the (001) bond (referred to as separation energy because of the calculation procedure used) of those layer-structure minerals that had well-determined crystal structures (Fig. 3). Values for lizardite, the platy serpentine mineral, were estimated from calculations of amesite (001) bond strength (Bish and Giese, 1981). The antigorite variety of serpentine should have a somewhat stronger (001) bond than lizardite, as sketched in Figure 3A. Dry platy minerals with

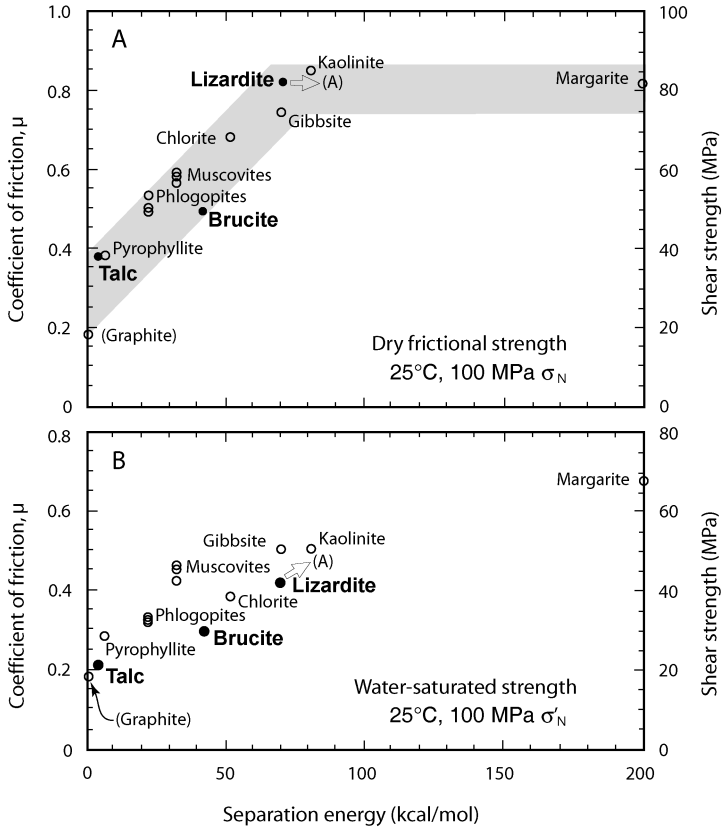

FIG. 3. Correlation of dry (A) and water-saturated (B) room-temperature frictional strengths of layer-structure minerals with the electrostatic (ionic) components of their (001) bonds (modified from Moore and Lockner, 2004). Bond-strength determinations are from Giese (1978, 1980) and Bish and Giese (1981). Graphite was added at 0 separation energy, because its crystal structure consists of layers of covalently bonded carbon atoms that are held together solely by weak van der Waals forces. Abbreviations: A = antigorite; its (001) bond should be somewhat stronger than that of lizardite, as indicated by the arrows.

separation energies ≥70 kcal/mole (Fig. 3A), such as lizardite, are characterized by $\mu \sim 0.8$. For those minerals whose separation energies are <70 kcal/mole, frictional strength is directly correlated with the interlayer-bond strength. Because of the localization of shear (Fig. 1C) and the preferred orientation of the platy grains subparallel to the shear planes, shear of the weaker gouges in Figure 3A (<70 kcal/mole) can occur by cleaving through the weak (001) bonds (Moore and Lockner, 2004). However, the (001) bonds of serpentine, kaolinite, and the brittle micas are strong enough that more energy would be required to shear through (001) than to initiate other frictional processes.

The water-saturated strengths of the layer-structure minerals also correlate directly with their interlayer bond strengths (Fig. 3B). Thin, structured water films are stabilized between the plate surfaces; such films can withstand normal stresses as high as several hundred MPa normal stress (Renard and Ortoleva, 1997), and they have a measurable shear strength that is a function of film thickness (Israelachvili et al., 1988). Moore and Lockner (2004) concluded that shear of water-saturated gouges of layer-structure minerals is concentrated in the water films. The shear strength of a given mineral is a function of the degree of attraction of the polar water molecules to the (001) surfaces, which in turn is correlated with factors that contribute to the electrostatic component of the bond (Fig. 3B).

Because shear strength increases with decreasing film thickness (Israelachvili et al., 1988),

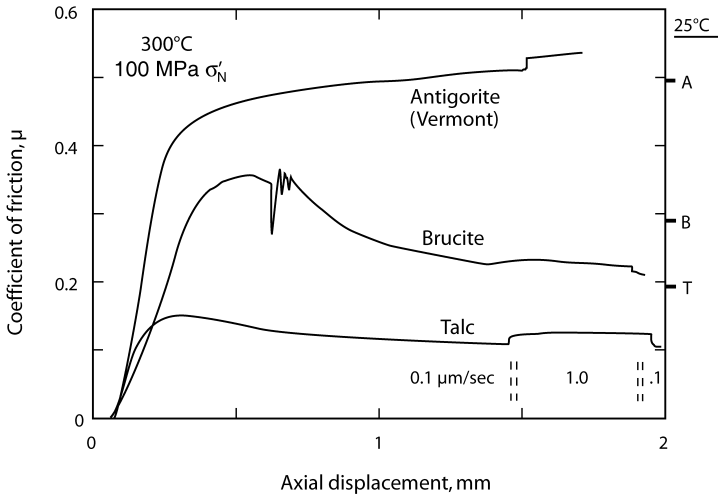

FIG. 4. Water-saturated frictional strengths of the Vermont antigorite, brucite, and talc at 300°C. Because corrections for the strength of the Cu-jackets are made after the experiments, the strength plots of heated samples appear to be shifted to the right of the origin. Final room-temperature values of μ for these minerals (at 8 mm axial displacement, Fig. 2) are plotted along the vertical axis at right, for comparison. Audible stress drops occurred during initial loading of several of the heated, water-saturated brucite samples.

increasing the effective normal stress should result in an increase in μ of layer-structure minerals toward their dry values. Such a relationship can be demonstrated for several layer-structure minerals, including montmorillonite, muscovite, biotite, chrysotile, kaolinite, chlorite, and talc (see review by Moore and Lockner, 2006), although the increase for talc is relatively small (Moore and Lockner, 2005b). Brucite, however, has a slightly negative stress dependence of μ at room temperature (Moore and Lockner, 2005a). Another influence on strength is increased salinity of the pore fluids, which causes the water films to collapse and tends to increase μ at low effective stresses (e.g., Kenney, 1967; Maio and Fenelli, 1994).

Strengths at Elevated Temperatures

Heating affects water-saturated antigorite, brucite, and talc differently (Fig. 4). Raising temperature from 25° to 300°C at constant effective normal stress causes antigorite to become somewhat stronger. In contrast, the coefficient of friction of brucite is about 30% lower and that of talc nearly 50% lower at 300°C than at room temperature. The factors that may control the high-temperature strength behavior of these minerals are discussed below.

Antigorite

The frictional strength of the New Idria antigorite increases steadily with temperature to 400°C (Fig. 5). In contrast, its dry strength at 300°C is the same as that for the Vermont antigorite measured at room temperature (Fig. 2). The water-saturated strengths of the New Idria antigorite and the relatively pure Vermont antigorite (Fig. 4) at 300°C are also essentially the same. Similar increases in μ with increasing temperature are shown by chrysotile to temperatures of 280°C (Moore et al., 2004) and by lizardite to 200°C (Moore et al., 1997). SEM images of New Idria antigorite samples (Fig. 6) illustrate the localization of shear onto boundary and R shears that is typical of gouges rich in layer-structure minerals. The gouge situated away from the shear surfaces shows little evidence of deformation. Textures of the heated samples are identical to those of samples deformed at room temperature. The temperature dependence of strength for the serpentine minerals is most easily explained in terms of changes in the water films between plates. Heating drives some of the water off the mineral surfaces, causing film thicknesses to decrease and shifting the strength toward the dry value.

Jacket failures limited the information collected on velocity (axial displacement rate) dependence of

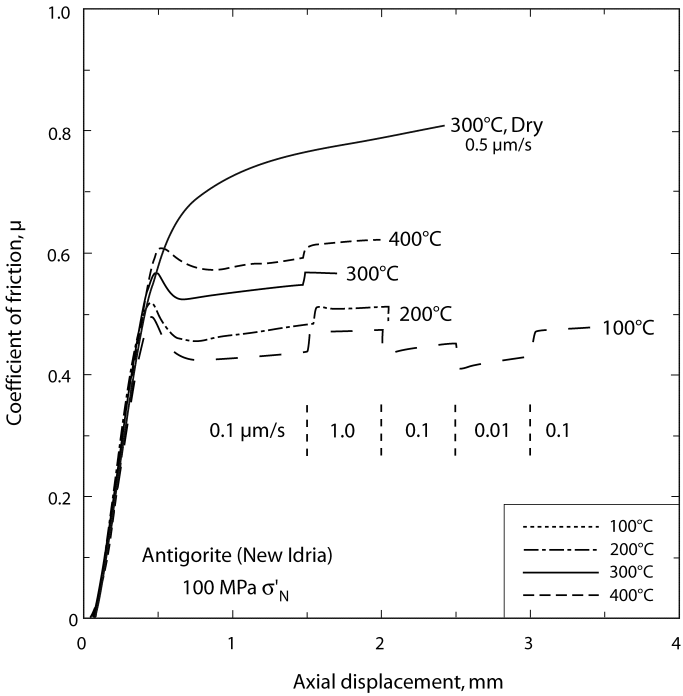

FIG. 5. Increase in μ with increasing temperature to 400°C for the water-saturated antigorite gouge from New Idria, California. Axial velocity was changed at intervals during the water-saturated experiments; antigorite is velocity-strengthening (μ increases with increasing velocity) over the limited range tested. The peaks in μ at <1 mm displacement may represent the work involved in forming the subsidiary shears. An additional experiment, run dry at 300°C, 100 MPa σ_N, and constant 0.5 μm/s axial velocity, is included for comparison.

strength. However, all of the antigorite experiments in Figures 4 and 5 are characterized by velocity-strengthening behavior (strength increases with increasing velocity), which is consistent with the results at 100°–200°C reported by Moore et al. (1997) for antigorite. In contrast, velocity data for heated lizardite and chrysotile are more variable. At a given temperature, lizardite shows both velocity-strengthening and velocity-weakening (strength decreases with increasing velocity) behavior over different velocity ranges (Moore et al., 1997). Chrysotile is largely velocity-strengthening at ~100°C and velocity-weakening at 280°C (Moore et al., 2004). Velocity-strengthening behavior permits stable slip, whereas velocity-weakening behavior is potentially unstable. The available data suggest that antigorite serpentinites may be more likely to shear aseismically than lower-temperature, lizardite ± chrysotile serpentinites.

Talc

Water-saturated talc becomes weaker with heating to 300°C (Fig. 7A). Strength then recovers somewhat at 400°C but remains within the range $0.10 \leq \mu \leq 0.15$. All of the velocity steps in Figure 7A indicate velocity-strengthening behavior, and talc is velocity-strengthening at all the conditions tested by Moore and Lockner (2005b).

To determine the cause of the weakening, experiments on oven-dried talc (Fig. 7B) were run at the same temperatures as the water-saturated experiments, but at a single velocity of 0.5 μm/s to match the dry 25°C experiment (Fig. 2). Dry talc follows the same trend as water-saturated talc, including the strength minimum at 300°C. The difference between the dry and water-saturated strengths of talc at each temperature was estimated, for comparison with serpentine. Because μ varies with velocity, differences between dry and wet strength should be determined at the same velocity. However, because

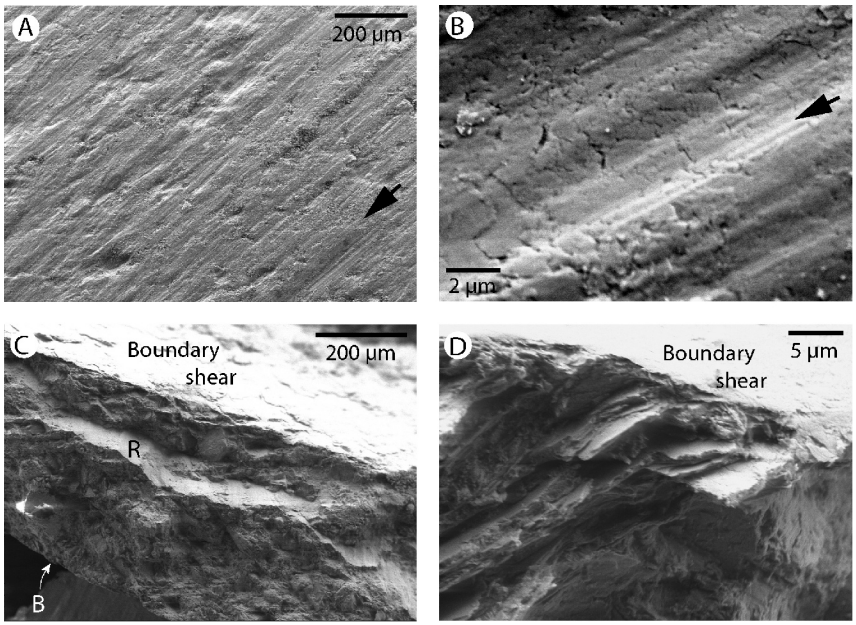

FIG. 6. Secondary-electron SEM images of the New Idria antigorite gouge. A. 300°C, 100 MPa σ'_N (50 MPa P_p). Striated boundary-shear surface; this is a finer-scale equivalent to the slickensided surfaces of many serpentinite rock samples. B. 400°C, 100 MPa σ'_N (50 MPa P_p). Cleavage flakes of antigorite lie flat on the shear surface. C. 100°C, 100 MPa σ'_N (50 MPa P_p). Cross section of gouge layer, showing the upper boundary-shear surface and part of an R shear. Gouge between the two shears has no preferred orientation and is less densely packed than the gouge forming the shears. D. Close-up of the boundary shear in C; antigorite grains bend into parallelism with the shear surface. This side of the boundary shear is ≤5 μm thick.

of the uniformly positive velocity dependence of μ for talc, the expected water-saturated strength at 0.5 μm/s will be bracketed between the values at 1.0 and 0.1 μm/s. Subtracting the values of water-saturated μ at 1.0 and 0.1 μm/s at the ~2 mm velocity step from the dry value at 2 mm yields the minimum and maximum values, respectively, for the change. The difference at room temperature, from Figure 2, is ~0.16. At 100°–200°C, the difference is bracketed between 0.10 and 0.12, and at 300°–400°C the difference is between 0.08 and 0.10.

Secondary-electron SEM images of shear surfaces from a dry talc experiment (Fig. 8A) and two water-saturated experiments (Figs. 8B and 8C) are very similar in appearance to each other and to the room-temperature talc sample depicted in Figure 1C. The textures of water-saturated talc also correspond to those of antigorite (Fig. 6). That the dry and water-saturated talc strengths change in tandem suggests that it is the strength of the (001) bond that is varying. Decreasing the interlayer bond strength makes it easier to shear through (001) of dry talc. It also lessens the attraction of water molecules to the plate surfaces, thereby reducing the shear strength of the water films between plates. As with serpentine, heating water-saturated talc appears to drive some water from the plate surfaces, bringing its strength closer to the dry value.

Brucite

Heated, water-saturated brucite follows a similar weakening trend to that of talc, reaching a minimum value of μ ~ 0.2 at 200–300°C (Fig. 9A). In contrast, dry brucite does not weaken at higher temperatures (Fig. 9B), and it is characterized by stick-slip motion, the sequence of stress drops and recoveries considered to be the laboratory equivalent of earthquakes. Some of the water-saturated brucite samples also had audible stress drops during initial loading. Those stress drops gradually diminished in intensity and ceased before the residual stress level was reached. The change in μ with velocity increase for heated brucite is typically 0 to slightly positive.

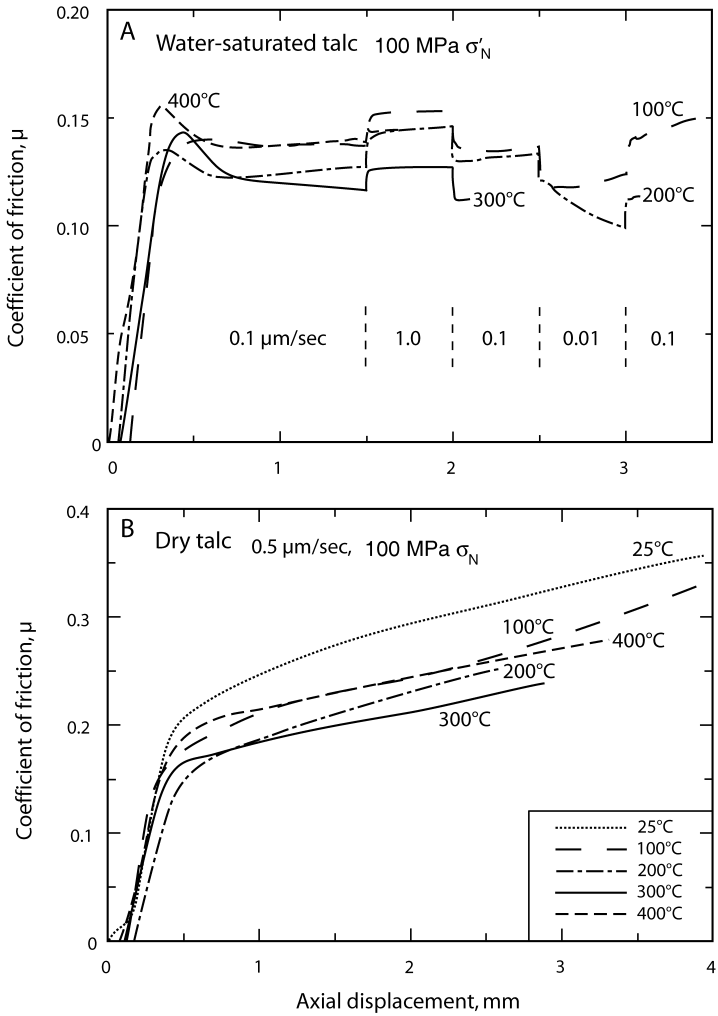

FIG. 7. Change in μ with temperature increase for heated talc at constant effective normal stress. A. Water-saturated talc; talc is velocity-strengthening at all conditions tested (Moore and Lockner, 2005b). B. Dry talc experiments conducted at a constant velocity of 0.5 μm/s. The 25°C test is the dry portion of the talc experiment in Figure 2.

Room-temperature brucite is largely velocity-weakening. SEM images of the brucite samples (Fig. 10) offer an explanation for its strength behavior. The deformation textures of sheared dry brucite (Figs. 10A and 10B) correspond to those of antigorite (Fig. 6) and talc (Fig. 8), but water-saturated brucite is characterized by extensive recrystallization along the boundary and R shears. The gouges in Figures 10C and 10D are from experiments that lasted 8 hours or less, and the samples were brought to room temperature within a few minutes of jacket failure. Solution-transfer processes clearly are involved in the shear of heated, water-saturated brucite, and they are the likely cause of its weakening. Brucite has high solubility and dissolution/precipitation rates (Jordan and Rammensee, 1996; Pokrovsky and Schott, 2004) that are several orders of magnitude greater than those for silicate minerals such as mica (e.g., Lin and Clemency, 1981). Water in the pores and in the films between plates provides a path for diffusional transfer of Mg ions away from high-stress sites (e.g., Renard and Ortoleva, 1997). Shear surfaces of the brucite samples have score marks of various sizes (Fig. 10C) that illustrate one

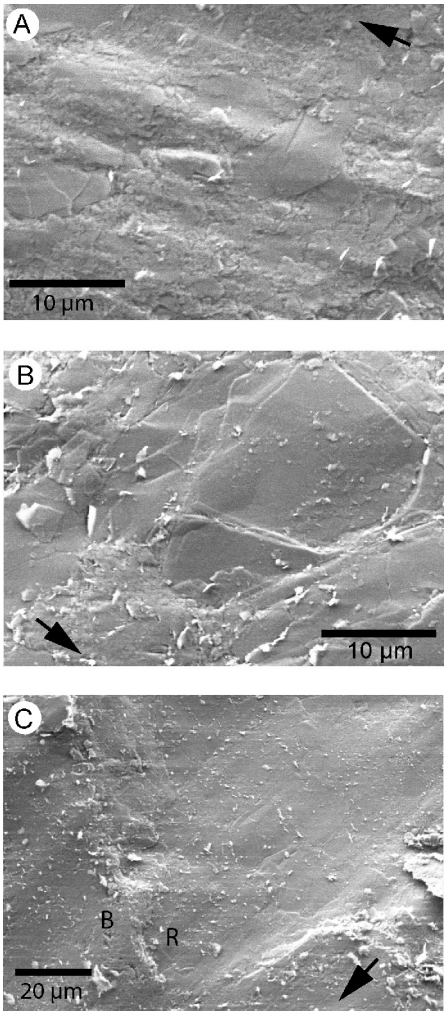

FIG. 8. In-lens secondary-electron SEM photos of shear surfaces in talc samples. A. 300°C, dry, 100 MPa σ_N. R shear with a slightly corrugated surface. B. 100°C, 100 MPa σ'_N (50 MPa P_p). R shear; platy grains on the shear surface are essentially identical in orientation and texture to those in the dry sample in A. C. 200°C, 150 MPa σ'_N (50 MPa P_p). Transition from an R shear at right to a boundary shear at left.

of the processes that may be occurring. These marks appear to have formed as a result of dissolution of brucite in front of an asperity on the opposite shear surface. The troughs are gradually filled with euhedral brucite (Fig. 10C).

Some of the other unusual features of brucite strength behavior may also be related in some way to pressure-solution processes. Examples include the slightly negative pressure dependence of μ for brucite at room temperature, and the stress drops during the early stages of shear of heated, water-saturated brucite.

Discussion

The strengths of antigorite, talc, and brucite gouges illustrate the variety of responses to heating that have been identified to date among individual layer-structure minerals. Their contrasting behavior also emphasizes the hazards of making generalizations about the strengths of the layer-structure minerals and of using room-temperature data to infer fault-zone properties at depth. The serpentine minerals and talc respond in the same way to heating in that the water-saturated coefficient of friction comes closer to the dry value. For talc, however, the dry value is not fixed, but rather shifts in response to temperature-dependent changes in (001) bond strength. Stress-induced solution-precipitation reactions dominate over other shearing processes for brucite, which has high solubility and rapid dissolution kinetics.

The high-temperature strength behavior of the serpentine minerals may be representative of several of the sheet silicates. Moore et al. (1986) reported substantial strength increases with heating for two water-saturated, clay-rich gouges. Each gouge contained about 80% clay minerals; the clay content of one was predominantly illite, and that of the other was about half montmorillonite and mixed-layer clays, with a substantial amount of kaolinite. The strength of a granodiorite gouge tested as part of the same study was essentially unaffected by heating; it was considerably stronger than the clay-rich gouges at 200°C but not at 400–600°C. Tembe et al. (unpubl. data) also measured large increases in μ with increasing temperature for an illite-rich fault gouge in core from the SAFOD (San Andreas Fault Observatory at Depth) drillhole.

In these short experiments, brucite was the only mineral to show obvious recrystallization textures, but over longer time periods fluid-assisted recrystallization may play an important role in shear deformation of other gouges. In addition, most of our recent work has focused on the behavior of individual minerals during shear. Mechanical mixtures of minerals from different sources, as in a mélange matrix, are likely to react to form new mineral assemblages in the presence of pore fluids. Strength and other physical properties might be affected by the ongoing reactions as well as the resulting changes in mineralogy.

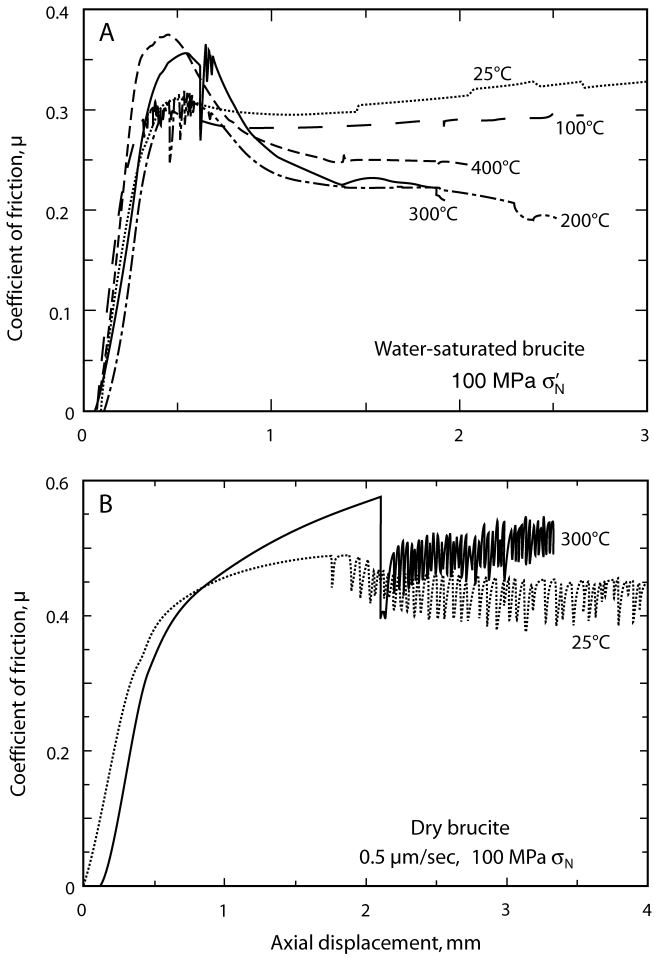

FIG. 9. Temperature dependence of μ for brucite at 100 MPa σ'_N. A. Water-saturated brucite. Velocity steps for the 25°C experiment are in the sequence: 1, 3.2, 10, 3.2, 1, and those at elevated temperatures vary between 0.01 and 1 μm/sec in the same sequence as used for heated antigorite and talc. After the recrystallization textures illustrated in Figures 10C and 10D were identified, the timing of the velocity steps was changed so all velocities could be included in a day-long experiment that was quenched immediately upon completion. B. Dry brucite. Both dry samples show stick-slip behavior after ~2 mm axial displacement. Legend is the same as in Figure 7.

Application to the Slab-Mantle Wedge Interface

A serpentinite mélange at the slab-mantle wedge interface will tend to migrate up the subduction thrust in response to its reduced density relative to overlying materials. The frictional strength of the materials in the mélange will be critically important to this upward movement and to the exhumation of HP/UHP rocks entrained in the mélange. Although they are somewhat weaker than the minerals they replace, the serpentine minerals are not particularly weak minerals. To achieve substantial weakening of serpentinite mélange requires some other mechanism such as elevated fluid pressure that reduces the effective normal stress and, consequently, the shear strength. Extensive mass transfer by aqueous fluids has been well documented in ultramafic mélange at the slab-mantle interface (e.g., Sorensen, 1988; Sorensen and Grossman, 1989), and nearly lithostatic fluid pressures have been inferred at the plate interface (e.g., Furukawa, 1993).

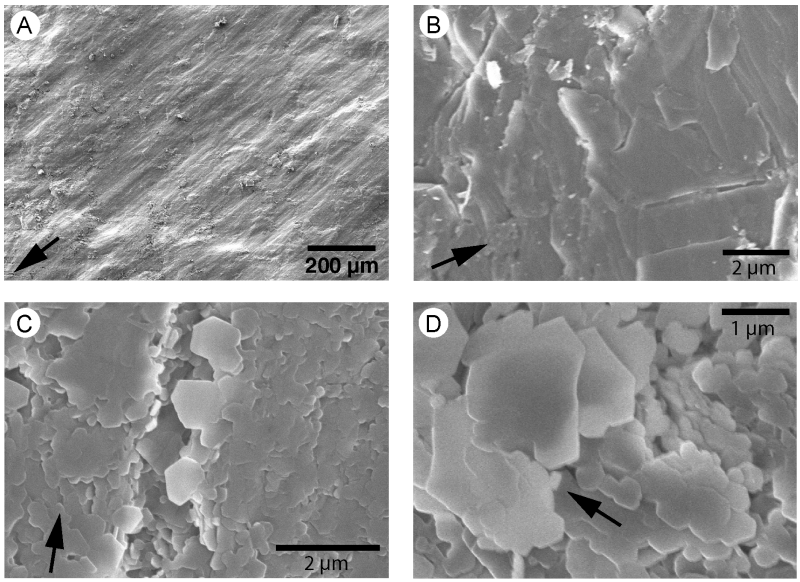

FIG. 10. Secondary-electron SEM photos of shear surfaces in brucite. A. 300°C, dry, 100 MPa σ_N. Low-magnification view of a corrugated boundary shear. B. 300°C, dry, 100 MPa σ_N. Boundary shear; brucite grains in the dry samples have the same appearance as dry and water-saturated talc in Figures 8A and 8B, respectively. C. 400°C, 100 MPa σ'_N (50 MPa P_p). Score mark on boundary shear; the top of the depression is partly covered by euhedral brucite. D. 300°C, 100 MPa σ'_N (50 MPa P_p). Boundary shear surface; coalesced platy crystals are elongate in the direction of shear. B–D are in-lens secondary-electron images.

Adding talc and brucite will also reduce the shear strength of serpentinized ultramafic rocks to varying degrees. Brucite forms as a byproduct of the serpentinization of olivine; complete serpentinization of a dunite will yield a maximum of 15–20% brucite. Brucite typically is disseminated in serpentinite (Hostetler et al., 1966), so the effect of brucite may be to reduce bulk shear strength by a small percentage (Moore et al., 2001). However, small amounts of brucite could potentially have a significant effect on strength, if the brucite can be concentrated along shear surfaces as a result of solution-transfer processes.

Talc may have a significant effect on deformation at the slab-mantle interface, because of its extreme weakness and because it is a constituent of subduction-zone ultramafic mélange at temperatures above the stability limit of serpentine (e.g., the amphibolite-facies unit of the Catalina Schist of California; Sorensen, 1988; Sorensen and Grossman, 1989; Bebout and Barton, 1989, 2002). Talc may be stable in subduction zones to depths of ~150 km (Pawley and Wood, 1995). Some talc will be disseminated in the mélange matrix, affecting the bulk shear strength in the same way as brucite. Talc is a common product of reaction between mafic and ultramafic mineral assemblages (Sanford, 1982). Mélange matrix that consists of a tectonic mixture of ultramafic rock from the mantle wedge and largely mafic rocks from the subducting slab will react to form talc-rich assemblages (e.g., Spaggiari et al., 2002). The involvement in the reactions of silica-rich fluids coming from the subducting slab will increase the talc content of the mélange matrix (Bebout and Barton, 2002).

Monomineralic talc layers can form as a result of metasomatism of ultramafic rocks over a wide range of metamorphic conditions (Sanford, 1982). The generation of a talc-rich zone along the hanging wall of the mantle wedge through progressive silica metasomatism, as hypothesized by Peacock and Hyndman (1999), would create a very weak zone that would effectively localize shear along the slab-mantle interface. Such a talc-rich zone has formed along the Trinity thrust, which represents a Devonian subduction zone that underlies mantle-wedge

rocks of the Trinity peridotite (Peacock, 1987). At a smaller scale, talc-rich layers form part of the reaction zones surrounding blocks entrained in subduction-zone mélange at blueschist-facies (Spaggiari et al., 2002) to amphibolite-facies conditions (Bebout and Barton, 2002). The local concentrations of talc potentially could affect the distribution of shear within the mélange matrix and the motion of the HP/UHP blocks relative to the matrix.

The focus of this paper has been on strength, but sliding stability is important for the estimation of earthquake hazard along subduction zones. Heated, water-saturated antigorite, talc, and brucite are velocity-strengthening over the range of conditions tested, indicating stable shear. This supports the contention of Peacock and Hyndman (1999) that hydrated mantle rocks at the interface with the subducting slab control the downdip limit of thrust earthquakes. The correlation between serpentinite and the seismic-aseismic transition may not be as good in cold subduction zones, where lizardite ± chrysotile would likely be present instead of antigorite, although talc and brucite are stable under those conditions.

Deep aseismic creep events, sometimes called slow or silent earthquakes, are associated with subduction of the Philippine Sea plate beneath Japan (Ozawa et al., 2002) and of the Juan de Fuca plate beneath northwestern North America (Miller et al., 2002). Slow slip events in the Cascadia subduction zone have been correlated with tremorlike seismic activity (Rogers and Dragert, 2003). The tremors initiate below the seismic-aseismic transition at 20–40 km depth, at or just above the plate boundary (Rogers and Dragert, 2003). The creep events can release large amounts of strain energy aseismically (Miller et al., 2002), but they may help to load the fault in the shallower, locked region and perhaps trigger great earthquakes (Ozawa et al., 2002; Rogers and Dragert, 2003). The locations suggest that the serpentinizing mantle wedge may play a role in the creep events and tremor. Further laboratory research to characterize processes at the slab-mantle interface may therefore be of use in assessing earthquake hazards of subduction zones.

Acknowledgments

This paper is written in honor of J. G. Liou, the first author's thesis adviser. S. Peacock and R. Simpson provided helpful reviews.

REFERENCES

Bebout, G. E., and Barton, M. D., 1989, Fluid flow and metasomatism in a subduction zone hydrothermal system: Catalina Schist terrane, California: Geology, v. 17, p. 976–980.

Bebout, G. E., and Barton, M. D., 2002, Tectonic and metasomatic mixing in a high-*T*, subduction-zone mélange—insights into the geochemical evolution of the slab-mantle interface: Chemical Geology, v. 187, p. 79–106.

Bish, D. L., and Giese, R. F., Jr., 1981, Interlayer bonding in IIb chlorite: American Mineralogist, v. 66, p. 1216–1220.

Byerlee, J. D., 1978, Friction of rocks: Pure and Applied Geophysics, v. 116, p. 615–626.

Coleman, R. G., 1980, Tectonic inclusions in serpentinites: Archives des Sciences, v. 33, p. 89–102.

Coleman, R. G., and Lanphere, M. A., 1971, Distribution and age of high-grade blueschists, associated eclogites, and amphibolites from Oregon and California: Geological Society of America Bulletin, v. 82, p. 2397–2412.

Dobretsov, N. L., and Buslov, M. M., 2004, Serpentinite mélanges associated with HP and UHP rocks in Central Asia, *in* Ernst, W. G., ed., Serpentine and serpentinites: Mineralogy, petrology, geochemistry, ecology, geophysics, and tectonics: Geological Society of America, International Book Series, v. 8, p. 119–142.

Evans, B. W., 2004, The serpentinite multisystem revisited: Chrysotile is metastable, *in* Ernst, W. G., ed., Serpentine and serpentinites: Mineralogy, petrology, geochemistry, ecology, geophysics, and tectonics: Geological Society of America, International Book Series, v. 8, p. 5–32.

Furukawa, Y., 1993, Depth of the decoupling plate interface and thermal structure under arcs: Journal of Geophysical Research, v. 98, p. 20,005–20,013.

Giese, R. F., Jr., 1978, The electrostatic interlayer force of layer structure minerals: Clays and Clay Minerals, v. 26, p. 51–57.

Giese, R. F., Jr., 1980, Hydroxyl orientations and interlayer bonding in amesite: Clays and Clay Minerals, v. 28, p. 81–86.

Guillot, S., Hattori, K. H., and de Sigoyer, J., 2000, Mantle wedge serpentinization and exhumation of eclogites: Insights from eastern Ladakh, northwest Himalaya: Geology, v. 28, p. 199–202.

Guillot, S., Hattori, K. H., de Sigoyer, J., Nägler, T., and Auzende, A.-L., 2001, Evidence of hydration of the mantle wedge and its role in the exhumation of eclogites: Earth and Planetary Science Letters, v. 193, p. 115–127.

Hostetler, P. B., Coleman, R. G., Mumpton, F. A., and Evans, B. W., 1966, Brucite in alpine serpentinites: American Mineralogist, v. 51, p. 75–98.

Hyndman, R. D., and Peacock, S. M., 2003, Serpentinization of the forearc mantle: Earth and Planetary Science Letters, v. 212, p. 417–432.

Israelachvili, J. N., McGuiggan, P. M., and Homola, A. M., 1988, Dynamic properties of molecularly thin films: Science, v. 240, p. 189–191.

Jordan, G., and Rammensee, W., 1996, Dissolution rates and activation energy for dissolution of brucite (001): A new method based on the microtopography of crystal surfaces: Geochimica et Cosmochimica Acta, v. 60, p. 5055–5062.

Kenney, T. C., 1967, The influence of mineral composition on the residual strength of natural soils, *in* Proceedings of the Geotechnical Conference on Shear Strength Properties of Natural Soils and Rocks, Oslo, Norway, 1967, p. 123–129.

Lin, F.-C., and Clemency, C. V., 1981, The kinetics of dissolution of muscovites at 25°C and 1 atm CO_2 partial pressure: Geochimica et Cosmochimica Acta, v. 45, p. 571–576.

Maio, C. D., and Fenelli, G. B., 1994, Residual strength of kaolin and bentonite: The influence of their constituent pore fluids: Géotechnique, v. 44, p. 217–226.

Manning, C. E., 1995, Phase-equilibrium controls on SiO_2 metasomatism by aqueous fluid in subduction zones: Reaction at constant pressure and temperature: International Geology Review: v. 37, p. 1039–1073.

Miller, M. M., Melbourne, T., Johnson, D. J., and Sumner, W. Q., 2002, Periodic slow earthquakes from the Cascadia subduction zone: Science, v. 295, p. 2423.

Moore, D. E., 1984, Metamorphic history of a high-grade blueschist exotic block from the Franciscan Complex, California: Journal of Petrology, v. 25, p. 126–150.

Moore, D. E., and Lockner, D. A., 2004, Crystallographic controls on the frictional behavior of dry and water-saturated sheet structure minerals: Journal of Geophysical Research, v. 109, B03401 [doi: 10.1029/2003JB002582], 16 p.

Moore, D. E., and Lockner, D. A., 2005a, Solution-transfer processes and the frictional strength of heated brucite [abs.]: EOS (Transactions of the American Geophysical Union), v. 86, fall meeting supplement, abstract T21B-0484.

Moore, D. E., and Lockner, D. A., 2005b, Talc friction at elevated temperatures and pressures: A very weak mineral throughout the seismogenic zone [abs.]: Geological Society of America Abstracts with Programs, v. 37, no. 7, p. 521.

Moore, D. E., and Lockner, D. A., 2006, Friction of the smectite clay montmorillonite: A review and interpretation of data, *in* Dixon, T. H., and Moore, J. C., eds., The seismogenic zone of subduction thrust faults: MARGINS, Theoretical and Experimental Earth Science Series, v. 2, in press.

Moore, D. E., Lockner, D. A., Iwata, K., Tanaka, H., and Byerlee, J. D., 2001, How brucite may affect the frictional properties of serpentinite: U.S. Geological Survey Open-File Report 01-320, 14 p.

Moore, D. E., Lockner, D. A., Ma, S., Summers, R., and Byerlee, J. D., 1997, Strengths of serpentinite gouges at elevated temperatures: Journal of Geophysical Research, v. 102, p. 14,787–14,801.

Moore, D. E., Lockner, D. A., Summers, R., Ma, S., and Byerlee, J. D., 1996, Strength of chrysotile-serpentinite gouge under hydrothermal conditions: Can it explain a weak San Andreas fault?: Geology, v. 24, p. 1041–1044.

Moore, D. E., Lockner, D. A., Tanaka, H., and Iwata, K., 2004, The coefficient of friction of chrysotile gouge at seismogenic depths, *in* Ernst, W. G., ed., Serpentine and serpentinites: Mineralogy, petrology, geochemistry, ecology, geophysics, and tectonics: Geological Society of America International Book Series, v. 8, p. 525–538.

Moore, D. E., Summers, R., and Byerlee, J. D., 1986, The effects of sliding velocity on the frictional and physical properties of heated fault gouge, *in* Wang, C.-y., ed., Internal structure of fault zones: Pure and Applied Geophysics, v. 124, p. 31–52.

Moore, D. E., Summers, R., and Byerlee, J. D., 1989, Sliding behavior and deformation textures of heated illite gouge: Journal of Structural Geology, v. 11, p. 329–342.

Morrow, C. A., Moore, D. E., and Lockner, D. A., 2000, The effect of mineral bond strength and adsorbed water on fault gouge frictional strength: Geophysical Research Letters, v. 27, p. 815–818.

Ozawa, S., Murakami, M., Kaidzu, M., Tada, T., Sagiya, T., Hatanaka, Y., Yarai, H., and Nishimura, T., 2002, Detection and monitoring of ongoing aseismic slip in the Tokai region, central Japan: Science, v. 298, p. 1009–1012.

Pawley, A. R., and Wood, B. J., 1995, The high-pressure stability of talc and 10Å phase: Potential storage sites for H_2O in subduction zones: American Mineralogist, v. 80, p. 998–1003.

Peacock, S. M., 1987, Serpentinization and infiltration metasomatism in the Trinity peridotite, Klamath province, northern California: Implications for subduction zones: Contributions to Mineralogy and Petrology, v. 95, p. 55–70.

Peacock, S. M., and Hyndman, R. D., 1999, Hydrous minerals in the mantle wedge and the maximum depth of subduction thrust earthquakes: Geophysical Research Letters, v. 26, p. 2517–2520.

Pokrovsky, O. S., and Schott, J., 2004, Experimental study of brucite dissolution and precipitation in aqueous solutions: Surface speciation and chemical affinity control: Geochimica et Cosmochimica Acta, v. 68, p. 31–45.

Renard, F., and Ortoleva, P., 1997, Water films at grain-grain contacts: Debye-Hückel, osmotic model of

stress, salinity, and mineralogy dependence: Geochimica et Cosmochimica Acta, v. 61, p. 1963–1970.

Rogers, G., and Dragert, H., 2003, Episodic tremor and slip on the Cascadia subduction zone: The chatter of silent slip: Science, v. 300, p. 1942–1943.

Sanford, R. F., 1982, Growth of ultramafic reaction zones in greenschist to amphibolite facies metamorphism: American Journal of Science, v. 282, p. 543–616.

Sorensen, S. S., 1988, Petrology of amphibolite-facies mafic and ultramafic rocks from the Catalina Schist, southern California: Metasomatism and migmatization in a subduction zone metamorphic setting: Journal of Metamorphic Geology, v. 6, p. 405–435.

Sorensen, S. S., and Grossman, J. N., 1989, Enrichment of trace elements in garnet amphibolites from a paleo-subduction zone: Catalina Schist, southern California: Geochimica et Cosmochimica Acta, v. 53, p. 3155–3177.

Spaggiari, C. V., Gray, D. R., and Foster, D. A., 2002, Blueschist metamorphism during accretion in the Lachlan orogen, south-eastern Australia: Journal of Metamorphic Geology, v. 20, p. 711–726.